Contents lists available at ScienceDirect

Carbohydrate Polymers

journal homepage: www.elsevier.com

Chemical structure and biological properties of sulfated fucan from the sequential extraction of subAntarctic *Lessonia* sp (Phaeophyceae)

D. Leal[a, *], A. Mansilla[b], B. Matsuhiro[a], M. Moncada-Basualto[a, c], M. Lapier[d], J.D. Maya[d], C. Olea-Azar[c], W.M. De Borggraeve[e]

[a] Departamento de Ciencias del Ambiente, Facultad de Química y Biología, Universidad de Santiago de Chile, Av. L. B. O'Higgins 3363, Santiago, Chile
[b] Laboratorio de Macroalgas Antárticas y Subantárticas, Universidad de Magallanes, Av. Bulnes 1465, Punta Arenas, and Instituto de Ecología y Biodiversidad, Chile
[c] Departamento de Química Inorgánica y Analítica, Universidad de Chile, Av. Sergio Livingstone 1007, Santiago, Chile
[d] Departamento de Farmacología Molecular y Clínica, Facultad de Medicina, Universidad de Chile, Av. Independencia 1107, Santiago, Chile
[e] Molecular Design and Synthesis, Department of Chemistry, KU Leuven, Celestijnenlaan 200F, Box 2404, 3001 Heverlee, Belgium

ARTICLE INFO

Keywords:
Fucoidan
Sulfated fucan
Antioxidant
Antiparasitic
Biological activities

ABSTRACT

This work is related to the structural characterization of the sulfated polysaccharide from *Lessonia* sp and the study of its antioxidant and antiparasitic properties. Sequential extraction afforded D-mannitol as the only low MW sugar alcohol. Extraction with 2% $CaCl_2$ afforded in 3.0% yield, a sulfated fucan (SF). Its major fraction (48.5% yield), isolated by ion-exchange chromatography corresponds to a linear polymer of α-L-fucopyranosil residues linked 1→3, sulfated at the *O*–4 and partially at *O*–2 positions. By alkaline extraction, sodium alginate (10.3% yield) was obtained. The antioxidant capacity of SF by ESR showed high elimination index (IC_{50}, mg/mL) of hydroxyl (0.27), alkoxy (10.05), and peroxyl (82.88) radicals in relation to commercial mannitol. SF showed activity against the epimastigote form of *Trypanosoma cruzi* parasite (250 μg/mL) and low cytotoxicity in murine cells (367 μg/mL). The elimination capacity of radicals in aqueous medium of SF would allow its potential biomedical application.

1. Introduction

This study is based on field detections of *Lessonia* individuals with a peculiar morphology in the southern part of the sub-Antarctic ecoregion of Magallanes. The morphotype had a typical *Lessonia* morphology and anatomy, with the emergence of several thick stipes from a massive holdfast of partially fused hapteria, bifurcated stipes that differentiate into flat laminae at their apical part. Blade and stipe have a central, filamentous medulla, extensive cortex of relatively small cells with mucilage cavities, and outer layer of meristoderm. The range distribution of the corrugated morphotype seems restricted to the southernmost coasts of the sub-Antarctic ecoregion of Magallanes.

The major polysaccharide produced by brown algae is alginic acid, a copolymer of β-D-mannuronic acid and α-L-guluronic acid (Haug, Larsen, & Smidsrød, 1974; Painter, 1983). Previously, it was found that alkaline extraction of *Lessonia* sp afforded sodium alginate with a mannuronic (M) to guluronic acid (G) ratio (M/G) of 1.29. Partial hydrolysis of the alginate showed that it was mainly composed of a homopolymannuronate fraction (52%), whereas alginate (M/G 1.51) obtained from *Macrocystis pyrifera* collected in the Magellan Region contained 30.4% homopolymannuronate fraction (Cárdenas-Jirón, Leal, Matsuhiro, & Osorio-Roman, 2011; Matsuhiro, Martínez-Gómez, & Mansilla, 2015). On the other hand, alginates from *Lessonia vadosa,* showed lower M/G ratios (0.33–0.90). However, only the alginate from seaweed samples collected in spring showed to be enriched in polyguluronic acid (55.7%) (Chandía, Matsuhiro, Mejias, & Moenne, 2004). In the case of *Lessonia flavicans* (M/G 1.03), partial hydrolysis of the alginate indicated the major presence of polymannuronate block fraction (41.3%) (Leal, Matsuhiro, Rossi, & Caruso, 2008). Besides alginic acid, brown seaweeds produce sulfated fucans, mainly composed of L-fucopyranosyl residues linked α1→3 and α1→4 bonds; in addition to substitution by hemi-ester sulfate groups, fucans may contain D-xylose, D-galactose, D-mannose, D-glucose and D-glucuronic acid (2004, Bilan et al., 2002; Chevolot, Mulloy, Ratiskol, Foucault, & Colliec-Jouault, 2001; Painter, 1983; Patankar, Oehninger, Barnett, Williams, & Clark,

* Corresponding author.
Email address: david.leal.r@usach.cl (D. Leal)

https://doi.org/10.1016/j.carbpol.2018.07.012
Received 15 May 2018; Received in revised form 29 June 2018; Accepted 4 July 2018
Available online xxx
0144-8617/

1993, 2017). According to Li, Lu, Wei, and Zhao, (2008), the term fucoidan refers to polysaccharides that contain L-fucose and sulfate groups. Sulfated fucans and fucoidans exhibit amongst other anticoagulant, anti-inflammatory, antitumor and antiviral properties (Ale, Mikkelsen, & Meyer, 2011; Berteau & Mulloy, 2003; Croci et al., 2011; Cunha & Grenha, 2016; Jiang et al., 2010; Nagumo & Nishino, 1996; Pomin & Mourão, 2008; Wijesinghe & Jeon, 2012). Lorbeer et al. (2017) have recently conducted the sequential extraction of four brown seaweeds from southern Australia, among them *M. pyrifera*. They reported that *M. pyrifera* contained alginic acid (12%) and a heteropolysaccharide (5.1%) mainly composed of fucose within 18.6% of sulfate groups. It is interesting to note that *M. pyrifera* collected in the Magellan Region, Chile, also produced sulfated polysaccharides (1.5%) whereas the major fraction (60%) was a fucoidan containing 32.9% of sulfate groups and 3.6% of uronic acids; 2D NMR spectroscopy studies suggested the presence of α1→3 linked fucopyranosyl residues completely sulfated at the *O*–2 position and partially substituted at the *O*–4 position by sulfate groups or 3-*O*-sulfated fucopyranosyl residues (Reyes, 2011). Likewise, sequential extraction of *L. vadosa* from Southern Chile showed to contain alginic acid (17.0%) and a sulfated fucan (2.9%) (Chandía, Matsuhiro, Ortiz, & Mansilla, 2005). On the other hand, extraction of *L. vadosa* with 2% aqueous $CaCl_2$ afforded a fucoidan with 37.7% of sulfate groups; solvolytic desulfation and free radical depolymerization of the native polysaccharide allowed to establish that it was mainly composed of 1→3 linked α-L-fucopyranosyl residues sulfated at the *O*–4 position and partially sulfated at the *O*–2 position. This fucoidan showed good anticoagulant activity and elicitor activity in tobacco plants (Chandía & Matsuhiro, 2008). In addition, the antioxidant capacity was assayed of native fucoidan from *L. vadosa*, as well as their partially depolymerized and over-sulfated derivatives; it was found by $ABTS^{\circ+}$, ORAC and scavenging activity towards hydroxyl radicals, that the sulfate group in the *O*–2 position should decrease the anomeric hydrogen bond energy and increase the hydrogen atom abstraction reaction rate (Barahona, Chandía, Encinas, Matsuhiro, & Zúñiga, 2011, 2014; Torres et al., 2014).

On the other hand, the biological activities of polysaccharides have been described, such as: anticoagulant, antithrombotic, antitumor, antiviral and anti-inflammatory properties, among others (Yu, Shen, Song, & Xie, 2018). However, the antiparasitic activity of sulfated polysaccharides has been little explored; despite this, it has been reported that sulfated polysaccharides of the red alga *Solieria filiformus* showed moderate activity against the parasite *Leishmania amazonensis* (Ringgeler & Kappes, 2016), and Spavieri et al. (2010) reported the antiprotozoal activity of a chloroform-methanol extract of some green seaweeds against *Trypanosoma cruzi* parasites. In addition, it has been described that the algae *Chondria* sp, *Sargassum vulgare*, and *Ulva* sp from Cuba, *Sargassum thunbergii* from Japan; and *Laurencia microcladia*, *Jania capillaceae*, *Dictyota caribaea* and *Sargassum fluttans* from the Gulf of Mexico have been used for their anti-helminthic and antiprotozoal properties in traditional medicine (Torres et al., 2014).

Despite the known potential use of sulfated polysaccharides against these parasites, the activity of sulfated fucans of brown algae against *T. cruzi* has not been described; this parasite is responsible for American trypanosomiasis or Chagas disease, endemic to South America and is regarded as a neglected tropical disease by WHO. In addition, this disease is associated with deficit socioeconomical aspects. The drugs available for the treatment of the disease nifurtimox (NFX) and benznidazole (BNZ) have low efficacy and adverse effects. Therefore, there is a need to study bioactive compounds with greater efficiency (Pérez-Molina & Molina, 2018).

The aim of this work is related to the structural characterization of the sulfated polysaccharide from the brown seaweed *Lessonia* sp and the study of its antioxidant and antiparasitic properties.

2. Experimental

2.1. Materials and methods

Lessonia sp (Ochrophyta, Phaeophyceae) was collected in Tekenika Bay (55°19′60″S, 68°25′0″W), southern Chile (Cárdenas-Jirón et al., 2011; Leal, De Borggraeve, Encinas, Matsuhiro, & Müller, 2013). Voucher specimens are housed at the herbarium of the Laboratorio de Macroalgas Antárticas y Subantárticas of the University of Magallanes, Punta Arenas, Chile; and an image of the alga is shown in Fig. 1a. The epimastigote Dm28c strain of *T. cruzi* and RAW 264.7 cells were obtained from an in house collection (Programa de Farmacología Molecular y Clínica, Facultad de Medicina, Universidad de Chile). Reagent grade chemicals were purchased from Sigma-Aldrich Chemical Co. (St. Louis, MO, USA) and solvents were purchased from Merck (Darmstadt, Germany). FT-IR spectra in KBr pellets (10% w/w) were recorded in the 4000–400 cm^{-1} region using a Bruker IFS 66*v* instrument (Billerica, MA, USA), second derivative spectra were acquired using the OPUS/IR v.1.44 software incorporated into the hardware of the instrument (Leal et al., 2008). NMR spectra of polysaccharides were recorded at 70 °C in

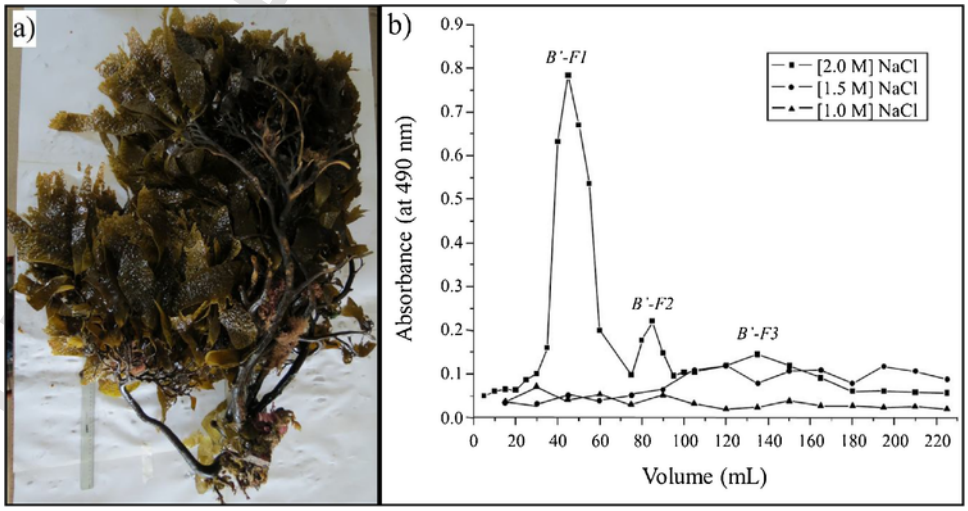

Fig. 1. *a)* Individual of *Lessonia* sp collected in the Beagle Channel, Biosphere Reserve Cape Horn (Chile). *b)* Elution profile on DEAE Sephadex A-50 chromatography (IEC) of the **B'** extract at different NaCl concentrations. **B'-F1** to **B'-F3** fractions, eluted at 2.0 M NaCl.

D_2O on a Bruker Avance II 600 spectrometer (Billerica, MA, USA) operating at 600.13 MHz (^{1}H NMR) and 150.90 MHz (^{13}C NMR) after isotopic exchange with D_2O, using the sodium salt of 3-(trimethylsylyl)-1-propionic 2,2,3,3-d_4 acid as internal reference (Leal et al., 2013). All two-dimensional experiments were acquired using a pulsed field gradient NMR sequences. The two-dimensional heteronuclear single quantum coherence correlation (^{13}C/^{1}H HSQC) spectra were acquired with 128×2040 data points and processed in a 1024×2048 matrix to give a final resolution close to 2.3 Hz point^{-1} in ^{1}H NMR and close to 2.4 Hz point^{-1} in ^{13}C NMR. Optical rotations were measured with a Perkin-Elmer 241 polarimeter (Waltham, MA, USA). Total sugars and uronic acids contents were determined according to Chaplin (1986), and Filisetti-Cozzi and Carpita (1991), respectively. Sulfate content was analyzed by the turbidimetric method of Dodgson and Price (1962). Gas–liquid chromatography (GLC) was carried out on a Shimadzu GC-14B chromatograph (Shimadzu Co., Kyoto, Japan) equipped with a flame ionization detector using a HP-ULTRA 2 (Agilent Technologies, Santa Clara, CA, USA) column (0.20 mm × 50 m×0.11 μm). ESR spectra were recorded in the X band (9.7 GHz) using an ECS 106 spectrometer (Bruker, Coventry, UK) with a rectangular cavity and 50 kHz field modulation, equipped with a high-sensitivity resonator at room temperature. Spectrometer conditions were: microwave frequency 9.81 GHz, microwave power 20 mW, modulation amplitude 0.91 G, receiver gain 59 db, time constant 81.92 ms and conversion time 40.96 ms (Robledo-O'Ryan et al., 2017). The fluorescence was measured with a Synergy™ HT multidetection microplate reader from Bio-Tek Instruments, Inc. (Winooski, VT, USA), using white polystyrene 96-well plates, purchased from Nunc (Roskilde, Denmark). Fluorescence was read from the top, with an excitation wavelength of 485/20 nm and an emission filter of 528/20 nm. The plate reader was controlled by Gen 5 software. The photolysis of the samples was carried out at room temperature with a deuterium lamp DH-2000-BAL from Ocean Optic, Inc. (Largo, FL, USA).

2.2. Sequential extraction

The dry seaweed blades (100 g) were stirred with petroleum ether (b.p. 50–60 °C) (2.0 mL/g), and the supernatant was concentrated in vacuo; the extraction process was repeated until no more residue was obtained in the concentrate. The seaweed blades were dried at room temperature for 72 h and treated with 1.6 L of 96% ethanol and 0.4 L of 37% aqueous formaldehyde, after 72 h the solid was decanted and air dried. Then, the dried alga was sequentially extracted (20 mL/g) with 80% aqueous ethanol at 25 and 70 °C (yielding extracts **A** and **A'**, respectively), followed by 2% aqueous $CaCl_2$ at 25 and 70 °C (yielding extracts **B** and **B'**, respectively), then with diluted HCl at pH 2.0 at 70 °C (extract **C**), and finally with 3% aqueous Na_2CO_3 at 50 °C (extract **D**) (Percival, Venegas Jara, & Weigel, 1983). Each supernatant with exception of the 80% aqueous ethanolic extracts was centrifuged and dialyzed against distilled water for 48 h using a Spectra/Por membrane with MWCO of 3500 Da (Spectrum Laboratories Inc., Rancho Dominguez, CA, USA). The extracts were concentrated in vacuo, poured over 0.5 L of 96% ethanol and centrifuged. The resulting solids were dissolved in the minimum volume of distilled water, and freeze-dried. The 80% aqueous ethanolic extracts (**A** and **A'**) were separately treated at 80 °C with charcoal and filtered. The filtered solution was concentrated in vacuo, and the resulting syrup was crystallized from 98% ethanol. The 2% $CaCl_2$ extracts were purified according to Chandía and Matsuhiro (2008); the purified extracts **B** and **B'**, were fractionated on a DEAE Sephadex A-50 column (33.5 x 3.0 cm) by elution with water followed by increasing concentrations of sodium chloride solutions. Elution was monitored with the phenol-sulfuric acid reagent (Chaplin, 1986). Fractions eluted at 1.0, 1.5 and 2.0 M NaCl were separately dialyzed (MWCO 3500 Da membrane) against distilled water, concentrated in vacuo and freeze-dried. A sample of the fraction that eluted at 2.0 M NaCl and **B'** were hydrolyzed and analyzed as alditol acetates by GLC (Chandía & Matsuhiro, 2008). The HCl solid extract (**C**) was purified and fractionated as the 2% $CaCl_2$ extracts. The 3% Na_2CO_3 solid extract (**D**) was dialyzed against distilled water and purified as previously reported (Venegas, Matsuhiro, & Edding, 1993). An aliquot of the purified material was hydrolyzed with formic acid and analyzed by HPLC (Chandía et al., 2004).

2.3. Antioxidant capacity assays

2.3.1. Oxygen radical antioxidant capacity-fluorescein (ORAC-FL)

The reaction was carried out in 75 mM sodium phosphate buffer (pH 7.4), in a 200 μL final volume. Fluorescein (FL, 40 nM, final concentration) and purified **B'** extract (SF, 0.01 – 0.4 mg/mL) solutions in phosphate buffer (pH 7.4) were placed in each well of a 96-well plate. The mixture was pre-incubated at 37 °C for 15 min, and 2,2′-azo-bis(2-amidinopropane) dihydrochloride (AAPH) solution (18 mM, final concentration) was added (Alarcón, Campos, Edwards, Lissi, & López-Alarcón, 2008). The microplate was immediately placed in the reader and automatically shaken prior to each reading. The fluorescence was recorded every 1 min for 80 min A blank with FL and AAPH using buffer instead of the SF solution was used in each assay. Five calibration solutions of commercial mannitol (1.0–5.0 mg/mL) as the antioxidant were also used in each assay. The inhibition capacity was expressed as ORAC-FL values and it was quantified by integration of the area under the fluorescence decay curve (AUC). All reaction mixtures were prepared in triplicate and at least three independent assays were performed for each sample. The ORAC-FL indexes were calculated as described by Pérez-Cruz et al. (2017).

2.3.2. Hydroxyl radical scavenging assay using electron spin resonance spectroscopy (ESR)

The reactivity of the SF against the hydroxyl radical was investigated using the photolytic method. The scavenging activity was estimated by comparing the intensity of the spin adduct signals formed by the reaction between the trap 5-diethoxyphosphoryl-5-methyl-1-pyrroline-*N*-oxide (DEPMPO) and the hydroxyl radical, in the absence (control) and presence of the SF and was expressed as half of the maximum inhibitory concentration (IC_{50}). To prepare the samples, 150 μL of phosphate buffer (pH 7.4) and 50 μL of SF were mixed, followed by the addition of 50 μL of DEPMPO spin trap (30 mM final concentration) and finally 50 μL of 30% hydrogen peroxide. The mixture was put in an ESR cell and the sample was photolyzed with a deuterium lamp (at 392 nm) at room temperature for ten minutes.

2.3.3. Determination of alkoxyl radicals generated by photolysis of AAPH using ESR spectroscopy

Antioxidant capacity against alkoxyl radicals generated by photolysis of AAPH in aqueous medium was monitored by spin trapping methodology (Matos et al., 2015). The solution of SF in phosphate buffer pH 7.4 at different concentrations was mixed with 5,5-dimethyl-1-pyrroline-*N*-oxide (DMPO) at concentration of 200 mM and AAPH in buffer medium at concentration of 20 mM. The mixture was photolyzed under the conditions previously described. Then, the ESR spectrum was recorded in the conditions described above. The antioxidant capacity was considered proportional to the decrease of signal height compared to the control in absence of antioxidant.

2.4. Cytotoxicity assay

The effect of SF on RAW 264.7 cells was evaluated with a 3[4,5-dimethylthiazol-2-yl]-2,5-diphenyltetrazolium bromide dye (MTT) assay as a viability test (Mosmann, 1983). The compound under study, dissolved in water, was added to the culture media at concentrations between 10–500 μg/mL. Next 10 μL of 5 mg/mL MTT plus 0.22 mg/mL phenazine metosulfate (electron carrier) were added at each well containing RAW 264.7 cell culture in 100 μL RPMI 1640. After incubation at 37 °C for 4 h, the generated water-insoluble formazan dye was dissolved by the addition of 100 μL of 10% w/v sodium dodecyl sulphate (SDS) in 0.01 M HCl. The plates were further incubated at 37 °C overnight, and optical density of the wells was determined using a microplate reader (Asys Expert Plus©, Asys Hitach, Austria) at 570 nm. Under these conditions, the optical density is directly proportional to the viable cell number in each well. All experiments were performed at least three times and data reported as means and their standard deviations from triplicate cultures. Results are reported as the half maximal inhibitory concentration (IC_{50}), regarding the control (cells in culture medium).

2.5. Epimastigote stage viability study

Trypanocidal activity was evaluated against the *T. cruzi* epimastigote stage (clone Dm28c). It was measured through the MTT assay using 0.22 mg/mL phenazine methosulfate (as an electron carrier). *T. cruzi* epimastigotes were grown at 28 °C in Diamond's monophasic medium with 4 μM hemin. Fetal calf serum was added to a final concentration of 5%. SF was dissolved in water (10–500 μg/mL), and added to 3×10^6 parasites/mL in RPMI 1640 culture medium at 28 °C for 4 h. Likewise, Nifurtimox was added as a positive control. Then, tetrazolium salt was added at a final concentration of 0.5 mg/mL, incubated at 28 °C for 4 h, solubilized with 10% SDS/0.1 mM HCl and incubated overnight. After incubation, the number of viable parasites was determined by absorbance measures at 570 nm in a multiwell plate reader (Asys Expert Plus). Untreated parasites were used as controls (100% of viability). Results are reported as half maximal inhibitory concentration (IC_{50}).

3. Results and discussion

3.1. Isolation and chemical characterization of ethanolic and aqueous extracts

From the ethanolic extracts and subsequent crystallization (**A** and **A'**, 1.4% and 1.8% yield on dry alga basis, respectively), crystals were isolated with a melting point of 164–166 °C and an optical rotation of $[\alpha]\ \frac{24}{D} = -0.30°$ (c. 1.0, water). The optical rotation of the purified ethanolic extract agrees with the published value (lit. $[\alpha]\ \frac{24}{D} = -0.30°$) (Hough & Richardson, 1967) and confirmed that D-mannitol is the only low-molecular weight carbohydrate synthesized by *Lessonia* sp. These results were similar to those reported by Percival et al. (1983) for *Lessonia nigrescens* and by Matsuhiro and Zambrano (1990) for L. *trabeculata,* and six times higher than that found in *L. vadosa* (Chandía et al., 2005).

The cold and 70 °C purified 2% aqueous $CaCl_2$ extracts (**B** and **B'**, 0.3% and 2.9% of dry alga, respectively) were fractionated by ion-exchange chromatography (IEC), they were firstly eluted with distilled water followed by increasing concentrations of sodium chloride solutions. Fig. 1b depicts the elution profile of the **B'** extract. The extracts (**B** and **B'**) showed the same elution profile. An irregular polydisperse fraction was recovered at 1.5 M (35.1%). In addition, one major fraction, **B'-F1** (48.5%), was obtained by IEC, at concentrations of 2.0 M NaCl, and two minor fractions **B'-F2** (6.7%) and **B'-F3** (9.7%) were collected at 2.0 M, with an 85% overall mass recovery of the loaded sample on the gel (Fig. 1b). The yield and composition of native extracts (**B**, **B'** and **C**) and fractions obtained from the **B'** extract are listed in Table 1.

In the fractionation of the $CaCl_2$ extract by IEC, no fractions were obtained by elution with distilled water which implies the absence of neutral laminaran type polysaccharides. According to Percival et al. (1983) and Chandía et al. (2005), in most species of the genus *Lessonia*, laminaran type polysaccharides were not found. Acid hydrolysis of the native extracts, **B** and **B'**, and fractions obtained by IEC of **B'** followed by GLC analysis of the corresponding alditol acetates showed that fucose is the major monosaccharide with traces of xylose and galactose. Acidic extract (**C**) showed similar values to those found for 2% aqueous $CaCl_2$ extracts with a higher presence of uronic acid but lower amount of sulfate content. Table 1 showed that the native $CaCl_2$ extract **B'** along with the major fraction **B'-F1** is mainly composed of fucose; furthermore, the high negative values for their optical rotations are indicative of the presence of L-fucose, in agreement to those previously studied by Bilan et al. (2002), 2004, Bilan, Grachev, Shashkov, Nifantiev, & Usov, 2006; Bilan et al., 2017 and Chandía and Matsuhiro (2008) for fucoidans from brown seaweeds species. The high content of sulfate ester groups in the major fraction is in agreement with the elution profile shown in Fig. 1. The low content of uronic acids in 2% $CaCl_2$ extracts indicates the high amount of sulfated polysaccharides in the native extracts. Moreover, according to the GLC analysis and amount of sulfate ester groups determined, the molar ratio of fucose and sulfate for the native extract **B'** (1.0:1.17) and for the major fraction **B'-F1** (1.0:1.21) indicates that the polysaccharide isolated from *Lessonia* sp blades is a fucoidan. Altogether, these results indicate that

Table 1
Yield and composition of 2% aqueous $CaCl_2$ (**B** and **B'**) and diluted HCl (**C**) extracts from the sequential extraction of *Lessonia* sp, and the major fractions obtained by ion-exchange chromatography (IEC) of **B'** extract.

Sample	Yield (%)[a]	Neutral monosaccharide (%)[b]			$-SO_3Na$ (%)[c]	Uronic acids (%)[d]	$[\alpha]_D$ (°)[e]
		Fuc	Xyl	Gal			
B	---	41.5	tr.	tr.	33.9±1.1	7.4±0.5	−129.2
B'	---	41.8	tr.	tr.	34.5±0.8	7.2±0.2	−129.8
B'-F1	48. 5	43.5	tr.	tr.	37.0±0.5	4.1±0.2	−136.7
C	---	44.1	tr.	tr.	30.4±0.6	14.7±0.4	−127.7

[a] Based on the total recovery mass by IEC fractionation of 2% aqueous $CaCl_2$ extract.
[b] Fuc = Fucose; Xyl = Xylose; Gal = Galactose; tr. = Traces (< 2%); n.d. = No detected.
[c] Sulfate content determined by the turbidimetric method of Dodgson and Price (1962).
[d] Uronic acids determined by the colorimetric method of Filisetti-Cozzi and Carpita (1991).
[e] Optical rotation (c. 0.8, water) at 23 °C.

Lessonia sp synthesizes a family of sulfated fucans with low content of uronic acids.

The extracts (**B** and **B'**) and the major fraction obtained by IEC (**B'-F1**), were characterized by spectroscopic methods. All native extracts and the major fraction showed the same signals with apparent similarity of intensities in the FT-IR spectra. Fig. 2a and 2b show the FT-IR spectrum and the second derivative spectrum for the major fraction **B'-F1**, respectively. Three characteristic bands were observed (Fig. 2a); a band between 1265–1261 cm^{-1} (ν S═O, symmetric), assigned to sulfate ester groups (–O–SO_3); another one between 852–854 cm^{-1} (δ C–O–S, asymmetric), which was assigned to sulfate group linked to axial secondary alcoholic group; and a band at 580 cm^{-1} (δ O–S–O, asymmetric). Furthermore, the band at 853 cm^{-1} is resolved in the second derivative spectrum into two signals (Fig. 2b) with a shoulder at 826 cm^{-1} (δ C–O–S, asymmetric) assigned to secondary equatorial sulfate groups which indicate that the majority of sulfate groups occupy positions C-4, and only the lesser part of sulfate is located at C-2 and/or C-3 of α-L-fucopyranosyl residues (Bilan et al., 2004). The spectra also showed minor bands assigned to uronic acids (1653–1651 cm^{-1}), and no bands attributed to proteins were found. FT-IR results are in agreement to those previously reported by Chandía and Matsuhiro (2008) for a regular fucoidan from L. *vadosa*.

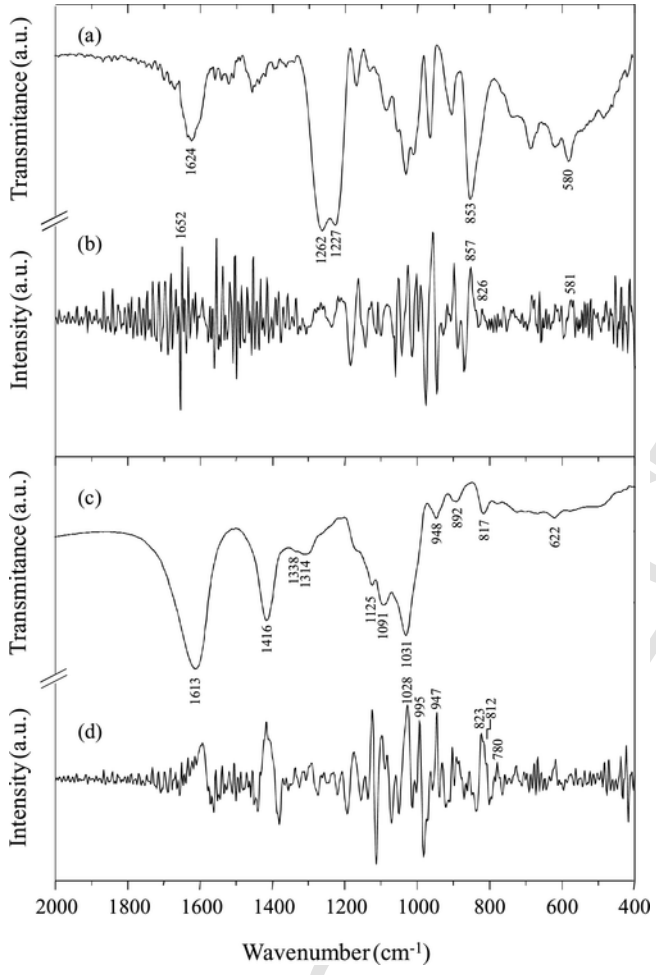

Fig. 2. *a)* FT-IR spectrum and *b)* second derivative spectrum in the 2000–400 cm^{-1} region of major fraction (**B'-F1**) obtained by IEC of 2% aqueous $CaCl_2$ extract. *c)* IR-TF spectrum and *d)* second derivative spectrum in the same region of the extract obtained by alkaline treatment with 3% Na_2CO_3 (**D**).

^1H and ^{13}C NMR and two-dimensional NMR spectra were collected in order to confirm the fine structure of extract **B'** and its major fraction (**B'-F1**). In these terms, ^1H and ^{13}C NMR spectra (not shown) presented the same spectral profile for both samples, showing two signals in the α-anomeric region and two signals assigned to methyl protons as shown in Table 2 for **B'-F1**. The structure of its major fraction **B'-F1** was accomplished with the aid of 2D NMR experiments and literature data (2006, Bilan et al., 2004).

$^1H/^1H$ COSY 2D NMR correlations (figure not shown) were in agreement to those reported for the fucoidan from *L. vadosa* (Chandía & Matsuhiro, 2008). Likewise **B'-F1** (Table 2), the native extract **B'** showed two different anomeric proton and H-2 correlations assigned to α-L-fucopyranosyl residues, H-1/H-2 (5.45/4.59 ppm) and H-1'/H-2' (5,37/3.96 ppm), indicating that the H-2 and H-2' protons correspond to sulfated residues at the *O*–2 position due to the sulfate ester group in this position generates the displacement towards low field of H-2. Integration of anomeric, H-4 and methyl protons (1.00:0.65:2.9) suggested that the fucoidan was partially sulfated at the *O*–2 position. Fig. 3a shows the $^{13}C/^1H$ HSQC 2D NMR spectrum of extract **B'**. It can be observed all $^1H/^{13}C$ correlations which could be assigned to →3-α-L-fucopyranosyl-2,4-di-*O*-sulfate residues (solid arrows) and to →3-α-L-fucopyranosyl-4-*O*-sulfate residues (dashed arrows). In addition, glycosidic linkages in the polysaccharide were analyzed by $^{13}C/^1H$ HMBC 2D NMR experiments (Fig. 3b), where α1→3 interactions (solid circles) are shown. Altogether these results indicate that *Lessonia* sp synthesizes a sulfated polysaccharide with the significance of a highly regular α1→3 fucoidan, completely sulfated at the *O*–4 position and partially sulfated at the *O*–2 position (Fig. 3c), similar to that obtained from *L. vadosa* (Chandía & Matsuhiro, 2008).

The 3% Na_2CO_3 extract **D** (26.1% of dry alga), after purification (10.3% of dry alga) showed in FT-IR spectroscopy and second derivative analysis (Fig. 2c and d, respectively) the characteristic bands at 948, 892, and 817 cm^{-1} (resolved at 822 and 812 cm^{-1} in the second derivative spectrum) which can be assigned to sodium alginate (Leal et al., 2013; Matsuhiro et al., 2015). Total hydrolysis with 90% HCOOH followed by HPLC analysis showed a mannuronic acid (M) to guluronic acid (G) ratio (M/G) of 1.38 ± 0.03; this value is very similar to that determined for the alginic acid obtained by direct extraction of blades with aqueous Na_2CO_3 (M/G = 1.31 ± 0.07) (Cárdenas-Jirón et al., 2011). It can be pointed out that the yield obtained for purified **D** ex-

Table 2
^1H and ^{13}C NMR data for major fraction (**B'-F1**) obtained by IEC of the 2% aqueous $CaCl_2$ extract at 70 °C.

Residue	Name	^1H and ^{13}C chemical shifts (ppm)					
1	→3)-α-L-Fuc*p*-2,4-diSO_3-(1→	***H-1***	***H-2***	***H-3***	***H-4***	***H-5***	***H-6***
		5.42	4.56	4.36	4.90	4.52	1.32
		C-1	***C-2***	***C-3***	***C-4***	***C-5***	***C-6***
		99.54	74.15	74.74	81.96	67.71	18.88
2	→3)-α-L-Fuc*p*-4-SO_3-(1→	***H-1'***	***H-2'***	***H-3'***	***H-4'***	***H-5'***	***H-6'***
		5.38	3.98	4.54	4.85	4.43	1.27
		C-1'	***C-2'***	***C-3'***	***C-4'***	***C-5'***	***C-6'***
		98.17	68.10	81.18	80.20	68.88	18.29

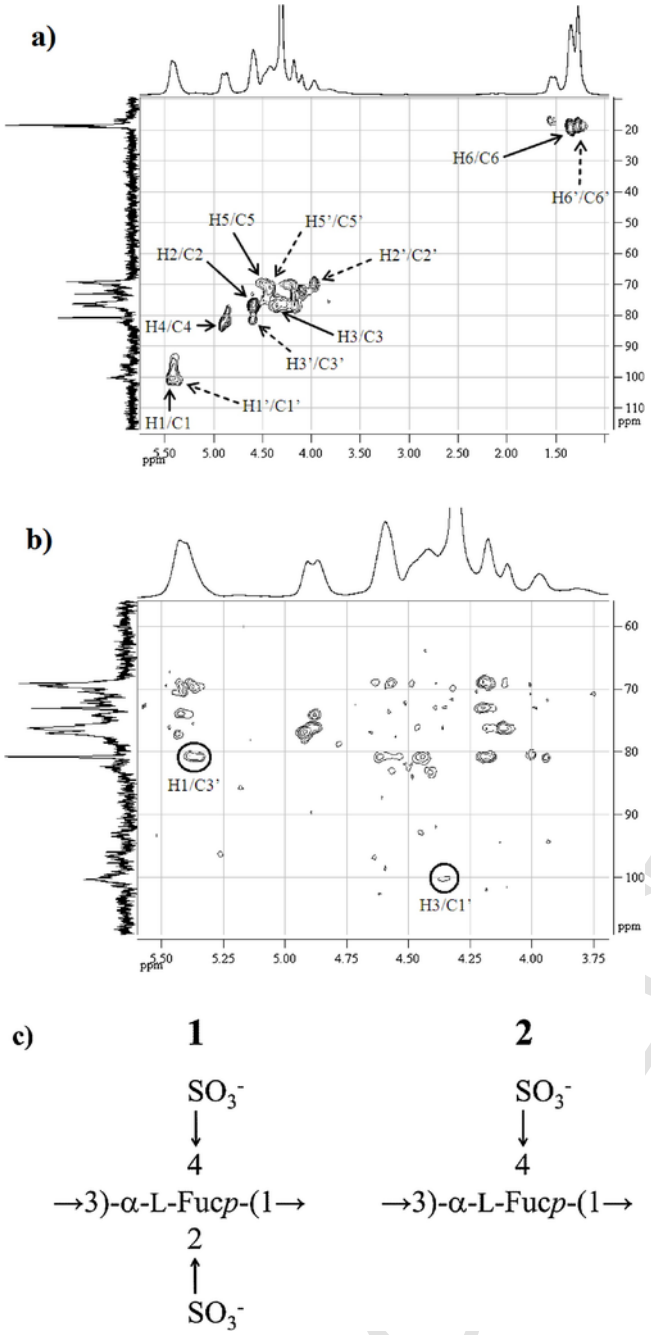

Fig. 3. Two dimensional $^{13}C/^{1}H$ NMR spectra (150/600 MHz) in D_2O at 70 °C of the native extract of 2% aqueous $CaCl_2$ (**B'**). *a)* HSQC NMR spectrum; Hx/Cx correspond to →3)-α-L-Fuc*p*-2,4-diSO_3-(1→ residues (solid arrows), and Hx'/Cx' correspond to →3)-α-L-Fuc*p*-4-SO_3-(1→ residues (dashed arrows). *b)* HMBC NMR spectrum; solid circles indicate the α1→3 glycosidic linkages. *c)* Representative diagram of the proposed structure for the predominant fucoidan synthesized by the brown seaweed *Lessonia* sp.

tract is lower than that obtained by direct extraction; this could be explained in terms of the several treatments of the alga in the sequential extraction. However, the total isolated amount of sodium alginate for *Lessonia* sp is about 30% higher than that obtained from other species from the *Lessonia* genus at the same season and 20% lower compared to *M. pyrifera* (Chandía, Matsuhiro, & Vásquez, 2001, 2004; Panikkar & Brasch, 1996; Percival et al., 1983).

3.2. Antioxidant capacity assays

3.2.1. Oxygen radical antioxidant capacity-fluorescein (ORAC-FL)

The peroxyl radical (ROO•) scavenging capacity towards the purified extract **B'** (SF), measured by the ORAC-FL method and taking commercial mannitol as reference (Kogan et al., 2005), was 10.05 ± 1.38. This value is higher than that found for the native fucoidan from *L. vadosa* and the sulfated galactan from the green variant of tetrasporic *Gigartina skottsbergii* (Rhodophyta) (Barahona, Encinas, Mansilla, Matsuhiro, & Zúñiga, 2012, 2014). However, these ORAC-FL index values were registered using as reference ascorbic acid, which exhibits different fluorescence decay kinetics. Furthermore, it was found that the ORAC values for sulfated polysaccharides, including commercial κ-, ι- and λ-carrageenans, did not correlate with the sulfate content. Likewise, Ajisaka, Oyanagi, Miyazaki, and Suzuki, 2016, b) reported a similar tendency for fucoidans extracted from several brown algae. Moreover, it was observed that the sulfated polysaccharides that presented the highest ORAC-FL values were the sulfated galactan from *Schizymenia binderi* and the fucoidan from *L. vadosa*, both with sulfation at the *O*–2 position of the glycopyranosyl residue (Barahona et al., 2014). If it is considered that the hydrogen abstraction occurs from the anomeric hydrogen of the internal monosaccharide units, the sulfate group in the *O*–2 position should decrease the hydrogen bond energy, and then increases the hydrogen atom abstraction reaction rate (Chen, Tsai, Huang, & Chen, 2009). In addition, it is known that the polysaccharide leads to an appreciated effect on the kinetic profile of the probe consumption, without an induction time, indicating that the polysaccharide display low activity to protect the fluorescein from the peroxyl radical. However, this may be related to the reactivity of SF and the formation of alkoxyl radical, more reactive than peroxyl radical, making difficult the rationalization and interpretation of the ORAC-FL values (Dorta et al., 2015). Therefore, it was decided in this work to directly study the elimination of peroxyl radicals of SF by means of electron spin resonance spectroscopy using the technique of spin trapping.

3.2.2. Alkoxyl radical scavenging

Kohri et al. (2009) introduced the ORAC-electron spin resonance (ESR) assay using the spin-trapping method for the determination of the AAPH-derived free radical. According to the authors, the ORAC-ESR assay is based on the competitive reaction between the spin-trapping of the AAPH-derived free radical, mainly RO•, and its elimination by antioxidant. ESR spin trapping provides a sensitive, direct and accurate method to monitor reactive species. In Fig. 4, it is shown that the photolysis of the azo compound AAPH generated the alkoxyl radical and the entrapment with the DMPO (spin trapp) was confirmed by the formation of four signals with the hyperfine coupling constants of the nitrogen (a_N = 14.27 G) and the hydrogen (a_H = 14.67 G) in the beta position of the cyclic nitrone (Nakajima, Matsuda, Masuda, Sameshima, & Ikenoue, 2012). Moreover, the formation of the spin-adduct between the peroxyl radical and the hydroxyl radical with the spin trap was not appreciated. The addition of increasing concentrations of the polysaccharide decreases the intensity of the signals in the ESR spectrum (Fig. 4a); from the relative intensity curve (Fig. 4b), the IC_{50} value was determined with a value of 0.36 ± 0.03 mg/mL, which is better than that found by Kim et al. (2014) for the fucoidan of *Ecklonia cava* (IC_{50} = 0.48 mg/mL). Additionally, commercial mannitol was used to determine the ORAC-EPR index value to compare this value with that determined through the ORAC-FL methodology.

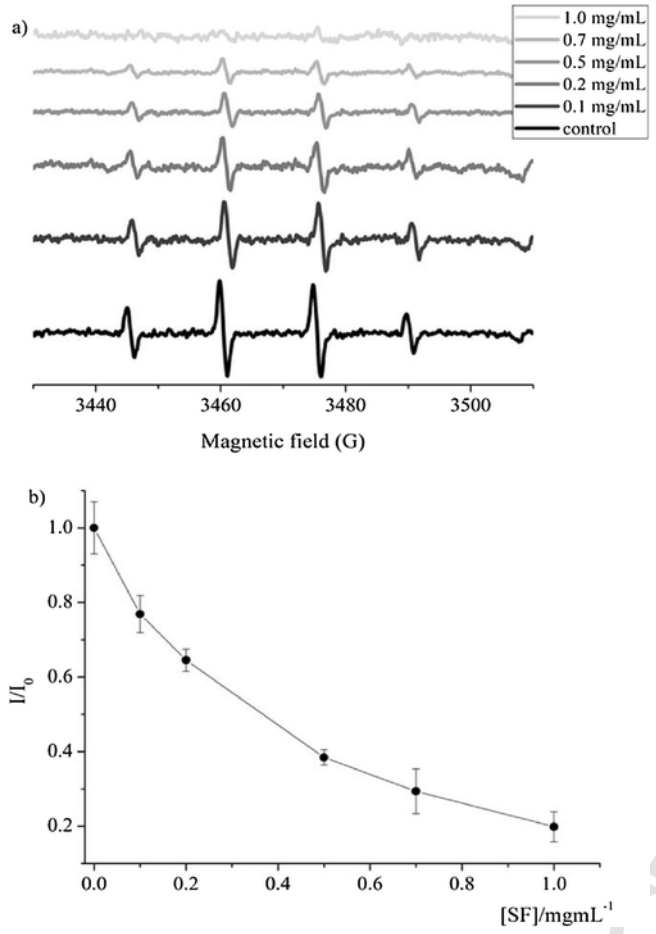

Fig. 4. *a)* Decrease in the intensity of the alkoxy radical signals in the ESR spectra by the addition of SF, *b)* Ratio between the normalized intensity in ESR spectra by the addition of SF.

$$RO\bullet + DMPO \xrightarrow{KST} [DMPO - OR]\bullet \quad (1)$$

$$RO\bullet + AOH \xrightarrow{KAOH} \text{Pr}\,oduct \quad (2)$$

If I_0 is the integration value of the signal in the absence of antioxidant and I the integration of the same signal in the presence of antioxidant (AOH), then I_0-I is proportional to the reaction rate in the presence of the antioxidant, while I is proportional to the reaction rate in the absence of antioxidant, in this way the relationship can be expressed:

$$\frac{I_0 - I}{I} = \frac{k_{AOH}}{k_{ST}} \times \frac{[RO^{\cdot}][AOH]}{[RO^{\cdot}][DMPO]} = \frac{k_{AOH}}{k_{ST}} \times \frac{[AOH}{[DMP}$$

$$\frac{I_0}{I} - 1 = \frac{k_{AOH}}{k_{ST}} \times \frac{[AOH]_0}{[DMPO]_0} \quad (4)$$

where $[AOH]_0$ and $[DMPO]_0$ denotes initial concentration of the component. A linear plot of (I_0/I)-1 against $[AOH]_0/[DMPO]_0$ provides the slope k_{AOH}/k_{DMPO} which is equal to the ORAC value for AOH relative to DMPO.

Since the kinetic constant of the reaction between the trap and the alkoxyl radical, k_{ST}, is common among all the compounds, an ORAC-ESR index is obtained by comparing the slopes (k_{AOH} / k_{ST}) of the commercial mannitol with SF polysaccharide (Fig. 5); slope values of 10.42 and 82.88 were obtained for commercial mannitol and SF, respectively. The ORAC-ESR index of SF was 7.95, lower than that obtained through ORAC-FL. This difference may be due to the fact that they correspond to different methodologies, while in the ORAC-ESR test the antioxidant capacity is measured by monitoring the concentration of the spin adduct generated with different increasing concentrations of antioxidant. The protection to the oxidation of a fluorescent probe in ORAC-FL is monitored over time by the effect of the addition of increasing concentrations of antioxidants; in other words, in the developed ORAC-ESR methodology, the antioxidant capacity was evaluated through the reactivity of the compound in competition with the spin trap, and in the ORAC-FL methodology, the stoichiometry of the reaction between the peroxyl radical (ROO•) and the donor of hydrogen atoms. This last point has been discussed, since it has been evidenced in ORAC-FL the formation of radicals RO• and ROO•, whose reactivities are different which makes it very difficult to rationalize and interpret the values of ORAC-FL (Dorta et al., 2017).

From these results, it is postulated that the antioxidant capacity of the purified extract **B'** (SF) from *Lessonia* sp, determined by hydrogen atom transfer methods, is more related to the stoichiometry of the reaction than to the reactivity of the polysaccharide towards the generated free radicals. The ORAC-ESR technique appears to be more effective than the ORAC-FL technique, since it allows the analysis of the structure of the generated radical and the decrease in the concentration of spin adduct. (Buettner, 1993; Kohri et al., 2009; Matos et al., 2015).

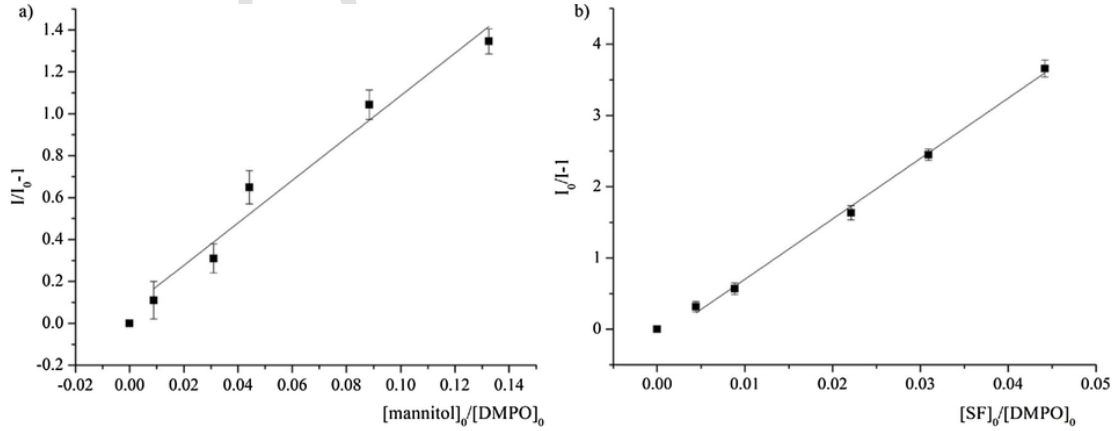

Fig. 5. Ratio between the intensity of the normalized signals of the ESR spectrum according to: *a)* concentration of commercial mannitol and the DMPO spin trap; *b)* concentration of SF and DMPO spin trap.

3.2.3. Hydroxyl radical scavenging

The capacity of elimination of the hydroxyl radical through ESR was studied, by means of the technique of spin trapping given that the hydroxyl radical has a half-life of 10^{-9} s (Davies, 2016; Villamena, 2017). The DEPMPO spin trap was used instead of the classic DMPO spin trap, since the former has a higher rate constant ($7.1\times10^{-9}\,M^{-1}s^{-1}$) for entrapping the hydroxyl radical. The entrapment of the hydroxyl radical was confirmed by the hyperfine coupling constants (a_N 14.1 G, $a_H = 13.2$ G and $a_P = 47.6$ G). The IC_{50} value was 0.27 mg/mL (Fig. 6), this result indicates that the SF is more active for the removal of the hydroxyl radical than the alkoxyl radical. Previously, the elimination of hydroxyl radical by sulfated polysaccharides was determined using other methodologies for the formation of the reactive species (Barahona et al., 2011, 2012, 2014; Sudharsan et al., 2015; Xu et al., 2017). The electron spin resonance in conjunction with the spin trapping technique ensures the formation of the hydroxyl radical, unlike other widely used tests. In addition, some assays use Fe^{2+} to catalyze the hydroxyl radical formation reaction. This may leads to a diminished antioxidant capacity due to chelation of the metal with the hydroxyl groups of the polysaccharide (Ajisaka, Oyanagi et al., 2016, b, Rendleman, 1978).

3.3. Cytotoxicity and trypanocidal activity

In the first place, cytotoxicity of SF from *Lessonia* sp was evaluated against mammalian cells (macrophages RAW 264.7 murine cells). The SF showed an IC_{50} value of 367 μg/mL ± 12. This activity was greater than that described for the native fucoidan of *L. vadosa*, the authors evidenced that fucoidan did not induce cytotoxic effects in dendritic cells in a concentration range between 10–1000 μg/mL (Barahona et al., 2014). Similarly, Yu et al. (2017) have recently shown that the modified sulfated polysaccharide of *Cyclocarya paliurus*, increase in the viability of macrophages RAW 264.7. The greater cytotoxicity of SF would be related to the lower degree of sulfation of the polysaccharide. It has been described that the introduction of sulfate groups could significantly increases the bioactivity of polysaccharides, including antioxidant and immunoregulatory activities (Nguyen et al., 2012).

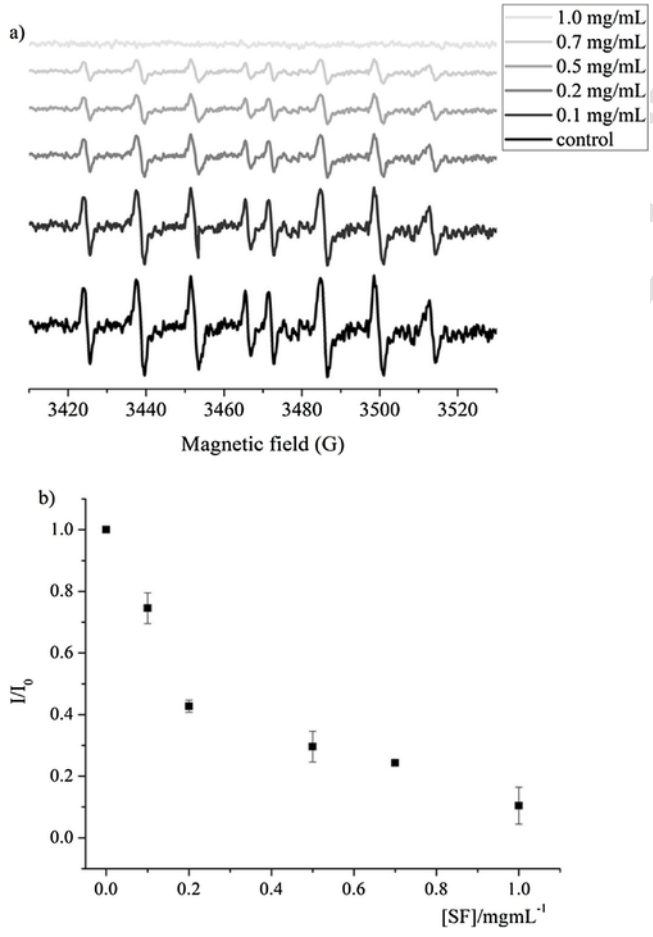

Fig. 6. *a)* Decrease in the intensity of the hydroxyl radical signals in the ESR spectra by the addition of SF, *b)* Ratio between the normalized intensity in ESR spectra by the addition of SF.

The trypanocidal activity was determined against the epimastigote form (non-infective replicative form) of the *T. cruzi* parasite, this form is found in the intestine of the transmitting insects and in the culture media. Likewise, the half maximal inhibitory concentration of the drug Nifurtimox, currently used for the treatment of Chagas disease, was determined (Robledo-O'Ryan et al., 2017).

The IC_{50} value of SF in the epimastigote form of *T. cruzi* was 250 μg/mL ± 3.92. The activity was lower than that determined for the Nifurtimox 28.84 μg/mL ± 1.34. Although SF was 8.9 times less active than Nifurtimox, the former has low cytotoxicity in mammalian cells, with an index of selectivity of 1.47 towards the parasite of *T. cruzi*. Therefore, the sulfated polysaccharides could be used as scaffolds for chemical modifications that increase the trypanocidal activity; such modifications could be related to the degree of sulfation of the polysaccharide.

A related point to consider is that the trypanocidal activity of sulfated polysaccharides against the *T. cruzi* parasite had not been described according to literature examination. Nevertheless, the trypanocidal activity of extracts of *Cladophora rupestris* and *Ulva lactuca* against *T. cruzi* has been described (IC_{50} values of 80.8 and 34.9 μg/mL) in which the activity can be attributed to the mixture of compounds in the extracts or to the synergy thereof (Spavieri et al., 2010).

Regarding the possible mechanism of antiparasitic action, it has been described that the activity of a commercial fucoidan against the intracellular form of the parasite *Leishmania donovani* induced a protective response to host cytokine and a significant increased ROS and NO levels in infected macrophages (Kar, Sharma, & Das, 2011). According to the literature mentioned, it is postulated that a possible mechanism would be related to the increase of ROS, generating oxidative stress in the parasite. The parasite of *T. cruzi* is deficient in endogenous antioxidant mechanisms, making them more susceptible to oxidative stress than mammalian cells (Aravena et al., 2011). Therefore, the use of sulfated polysaccharides would be an efficient strategy for the treatment of the infection.

The antioxidant capacity of SF would indicate that this polysaccharide could partially decrease the concentration of ROS or other reactive species, such as free radicals in biological medium. This would lead to a decrease in the trypanocidal activity of SF by the proposed mechanism. The inverse relationship between the trypanocidal activity and the antioxidant capacity has been previously described for anti-chagasic coumarins (Figueroa et al., 2013; Robledo-O'Ryan et al., 2017). Nevertheless, the structure of SF could be used as scaffolding for chemical modifications, considering the low toxicity in mammalian cells. These modifications should consider the decrease in antioxidant capacity and the increase in trypanocidal activity due to oxidative stress.

4. Conclusions

The species *Lessonia* sp presents similar characteristics to species of the genus *Lessonia* and *Macrocystis* in relation to content and chemical characteristics of the extracted polysaccharides. Sodium alginate of *Lessonia* sp blades is enriched on β-D-mannopyranuronic acid and is potentially interesting as industrial extraction source.

From the chemical, physical, spectroscopic and chromatographic studies of the 2% aqueous $CaCl_2$ native extract and its homogenous fraction, it is postulated that the *Lessonia* sp synthesizes a complex sulfated fucans, being the most important fraction a regular linear fucoidan, linked α1→3, completely sulfated at the *O*–4 position and partially sulfated at the *O*–2 position. Results obtained in this work indicate that the structural features of the fucoidan are similar to the obtained from L. *vadosa* collected at the same season and the same region.

The ESR in conjunction with the spin trapping technique is an efficient method for studying SF reactivity of *Lessonia* sp against free radicals centered on oxygen. The high capacity of elimination of radicals centered in oxygen in aqueous medium of SF, would allow its potential application in the pharmaceutical and food industry.

The trypanocidal activity determined for the first time against the *T. cruzi* parasite, allows to postulate that SF could be used as scaffolds for chemical modifications that increase the trypanocidal activity, considering that they are biodegradable systems with low cytotoxicity in mammalian cells.

Acknowledgments

The financial support of DICYT, Universidad de Santiago de Chile and the project U-REDES URC-024-16, Universidad de Chile is gratefully acknowledged.

References

Ajisaka, K., Oyanagi, Y., Miyazaki, T., Suzuki, Y., 2016. Effect of the chelation of metal cation on the antioxidant activity of chondroitin sulfates. Bioscience, Biotechnology, and Biochemistry 80 (6), 1179–1185.

Ajisaka, K., Yokoyama, T., Matsuo, K., 2016. Structural characteristics and antioxidant activities of fucoidans from five brown seaweeds. Journal of Applied Glycoscience 63, 31–37.

Alarcón, E., Campos, A.M., Edwards, A.M., Lissi, E., López-Alarcón, C., 2008. Antioxidant capacity of herbal infusions and tea extracts: A comparison of ORAC-fluorescein and ORAC-pyrogallol red methodologies. Food Chemistry 107, 1114–1119.

Ale, M.T., Mikkelsen, J.D., Meyer, A.S., 2011. Important determinants for fucoidan bioactivity. A critical review of structure-function relation and extraction methods for fucose containing sulfated polysaccharides from brown seaweeds. Marine Drugs 9 (10), 2106–2130.

Aravena, M., Olea, C., Cerecetto, H., González, M., Maya, J.D., Rodríguez-Becerra, J., 2011. Potent 5-nitrofuran derivatives inhibitors of Trypanosoma cruzi growth: Electrochemical, spectroscopic and biological studies. Spectrochimica Acta Part A: Molecular and Biomolecular Spectroscopy 79 (2), 312–319.

Barahona, T., Chandía, N.P., Encinas, M.V., Matsuhiro, B., Zúñiga, E.A., 2011. Antioxidante capacity of sulfated polysaccharide from seaweeds. A kinetic approach. Food Hydrocolloids 25, 529–535.

Barahona, T., Encinas, M.V., Mansilla, A., Matsuhiro, B., Zúñiga, E.A., 2012. A sulfated galactan with antioxidant capacity from the green variant of tetrasporic Gigartina skottsbergii (Gigartinales, Rhodophyta). Carbohydrate Research 347, 114–120.

Barahona, T., Encinas, M.V., Imarai, M., Mansilla, A., Matsuhiro, B., Torres, R., et al., 2014. Bioactive polysaccharides from marine algae. Bioactive Carbohydrates and Dietary Fibre 4, 125–138.

Berteau, O., Mulloy, B., 2003. Sulfated fucans, fresh perspectives: Structure, functions, and biological properties of sulfated fucans and an overview of enzymes active toward this class of polysaccharides. Glycobiology 13, 29–40.

Bilan, M.I., Grachev, A.A., Ustuzhanina, N.E., Shashkov, A.S., Nifantiev, N.E., Usov, A.I., 2002. Structure of a fucoidan from the brown seaweed F*ucus evanescens*. Carbohydrate Research 337, 719–730.

Bilan, M.I., Grachev, A.A., Ustuzhanina, N.E., Shashkov, A.S., Nifantiev, N.E., Usov, A.I., 2004. A highly regular fraction of a fucoidan from the brown seaweed Fucus distichus L.. Carbohydate Research 339, 511–517.

Bilan, M.I., Grachev, A.A., Shashkov, A.S., Nifantiev, N.E., Usov, A.I., 2006. Structure of a fucoidan from the brown seaweed Fucus serratus L.. Carbohydrate Research 341, 238–245.

Bilan, M.I., Ustyuzhanina, N.E., Shashkov, A.S., Thanh, T.T.T., Bui, M.L., Tran, T.T.V., et al., 2017. Sulfated polysaccharides of the Vietnamese brown alga Sargassum aquifolioum (Fucales, Sargassacea). Carbohydrate Research 449, 23–31.

Buettner, G.R., 1993. The pecking order of free radicals and antioxidants: Lipid peroxidation, α-tocopherol, and ascorbate. Archives of Biochemistry and Biophysics 300 (2), 535–543.

Cárdenas-Jirón, G., Leal, D., Matsuhiro, B., Osorio-Roman, I.O., 2011. Vibrational spectroscopy and density functional theory calculations of poly-D-mannuronate and heteropolymeric fractions from sodium alginate. Journal of Raman Spectroscopy 42, 870–878.

Chandía, N.P., Matsuhiro, B., 2008. Characterization of a fucoidan from Lessonia vadosa (Phaeophyta) and its anticoagulant and elicitor properties. International Journal of Biological Macromolecules 42, 235–240.

Chandía, N.P., Matsuhiro, B., Vásquez, A., 2001. Alginic acid in Lessonia trabeculata: Characterization by formic acid hydrolysis and FT-IR spectroscopy. Carbohydrate Polymers 46, 81–87.

Chandía, N.P., Matsuhiro, B., Mejias, E., Moenne, A., 2004. Alginic acid in Lessonia vadosa: Partial hydrolysis and elicitor properties of the polymannuronic acid fraction. Journal of Applied Phycology 16, 127–133.

Chandía, N.P., Matsuhiro, B., Ortiz, J.S., Mansilla, A., 2005. Carbohydrates from the sequential extraction of Lessonia vadosa (Phaeophyta). Journal of Chilean Chemical Society 50 (2), 501–504.

Chaplin, M.F., 1986. Monosaccharides. In: Chaplin, M.F., Kennedy, J.F. (Eds.), Carbohydrate analysis, a practical approach. IRL Press, Oxford; Washington, DC, pp. 1–36.

Chen, S.K., Tsai, M.L., Huang, J.R., Chen, R.H., 2009. In vitro antioxidant activities of low-molecular-weight polysaccharides with various functional groups. Journal of Agricultural and Food Chemistry 57, 2699–2704.

Chevolot, L., Mulloy, B., Ratiskol, J., Foucault, A., Colliec-Jouault, S., 2001. A disaccharide repeat unit is the major structure in fucoidans from two species of brown algae. Carbohydrate Research 330, 529–535.

Croci, D.O., Cumashi, A., Ushakova, N.A., Preobrazhenskaya, M.E., Picoli, A., Totani, L., et al., 2011. Fucans but not fucomannoglucuronans, determine the biological activities of sulfated polysaccharides from Laminaria saccharina brown seaweed. Plos One 6 (2), e17283, Doi: 10,1371/jpournal.pone.0017283..

Cunha, L., Grenha, A., 2016. Sulfated seaweed polysaccharides as multifunctional materials in drug delivery applications. Marine Drugs 14, 42. https://doi.org/10.3390/md14030042.

Davies, M.J., 2016. Detection and characterisation of radicals using electron paramagnetic resonance (EPR) spin trapping and related methods. Methods 109, 21–30.

Dodgson, K., Price, R., 1962. A note on the determination of the ester sulphate content of sulphated polysaccharides. Biochemical Journal 84, 104–110.

Dorta, E., Fuentes-Lemus, E., Aspee, A., Atala, E., Speisky, H., Bridi, R., et al., 2015. The ORAC (oxygen radical absorbance capacity) index does not reflect the capacity of antioxidants to trap peroxyl radicals. RSC Advances 5, 39899–39902.

Dorta, E., Aspée, A., Pino, E., González, L., Lissi, E., López-Alarcón, C., 2017. Controversial alkoxyl and peroxyl radical scavenging activity of the tryptophan metabolite 3-hydroxy-anthranilic acid. Biomedicine & Pharmacotherapy 90, 332–338.

Figueroa, R., Matos, M., Vazquez-Rodriguez, S., Santana, L., Uriarte, E., Olea-Azar, C., et al., 2013. Synthesis and evaluation of antioxidant and trypanocidal properties of a selected series of coumarin derivatives. Future Medicinal Chemistry 5 (16), 1911–1922.

Filisetti-Cozzi, T.M.C.C., Carpita, N.C., 1991. Measurement of uronic acids without interference from neutral sugars. Anaytical Biochemistry 197, 157–162.

Haug, A., Larsen, B., Smidsrød, O., 1974. Uronic acid sequence in alginate from different sources. Carbohydrate Research 32, 217–225.

Hough, L., Richardson, A.C., 1967. Penta-, hexa- and higher polyhydric alcohols. In: Coffey, S. (Ed.), Rodd's chemistry of carbon compounds, vol. I. Elsevier, New York, pp. 18–24.

Jiang, Z., Okimura, T., Yokose, T., Yamasaki, Y., Yamaguchi, K., Odata, T., 2010. Effects of sulfated fucan, ascophyllan, from the brown alga Ascophyllum nodosum on various cell lines. A comparative study on ascophyllan and fucoidan. Journal of Bioscience and Bioengineering 110, 113–117.

Kar, S., Sharma, G., Das, P.K., 2011. Fucoidan cures infection with both antimony-susceptible and -resistant strains of Leishmania donovani through Th1 response and macrophage-derived oxidants. Journal of Antimicrobial Chemotherapy 66 (3), 618–625.

Kim, E., Lee, S., Ko, C., Cha, S., Kang, M., Kang, S., et al., 2014. Protective effect of fucoidan against AAPH-induced oxidative stress in zebrafish model. Carbohydrate Polymers 102, 185–191.

Kogan, G., Staško, A., Bauerová, K., Polovka, M., Šoltés, L., Brezová, V., et al., 2005. Antioxidant properties of yeast (1→3)-β-D-glucan studied by electron paramagnetic resonance spectroscopy and its activity in the adjuvant arthritis. Carbohydrate Polymers 61 (1), 18–28.

Kohri, S., Fujii, H., Oowada, S., Endoh, N., Sueishi, Y., Kusakabe, M., et al., 2009. An oxygen radical absorbance capacity-like assay that directly quantifies the antioxidant's scavenging capacity against AAPH-derived free radicals. Analytical Biochemistry 386, 167–171.

Leal, D., Matsuhiro, B., Rossi, M., Caruso, F., 2008. FT-IR spectra of alginic acid block fractions in three species of brown seaweeds. Carbohydrate. Research 343, 308–316.

Leal, D., De Borggraeve, W., Encinas, M.V., Matsuhiro, B., Müller, R., 2013. Preparation and characterization of hydrogels based on homopolymeric fractions of sodium alginate and PNIPAAm. Carbohydrate Polymers 92, 157–166.

Li, B., Lu, F., Wei, X., Zhao, R., 2008. Fucoidan: Structure and bioactivity. Molecules 13 (8), 1671–1695.

Lorbeer, A.J., Charoensiddhi, S., Lahnstein, J., Lars, C., Franco, C.M.M., Bulone, V., et al., 2017. Sequential extraction and characterization of fucoidans and alginates from Ecklonia radiata, Macrocystis pyrifera, Durvillaea potatorum, and Seirococcus axillaris. Journal of Applied Phycology 29 (3), 1515–1526.

Matos, J.M., Mura, F., Vazquez-Rodriguez, S., Borges, F., Santana, L., Uriarte, E., et al., 2015. Study of coumarin-resveratrol hybrids as potent antioxidant compounds. Molecules 20 (2), 3290–3308.

Matsuhiro, B., Martínez-Gómez, F., Mansilla, A., 2015. Vibrational spectroscopy characterization of sodium alginate and its heteropolymeric and homopolymeric block fractions. In: Moore, A. (Ed.), Alginic acid: Chemical structure, uses and health benefits. Nova Science Publishers, New York, pp. 89–103.

Matsuhiro, B., Zambrano, D.M., 1990. Carbohydrate constituents of Lessonia trabeculata. Journal of Applied Phycology 2, 183–185.

Mosmann, T., 1983. Rapid colorimetric assay for cellular growth and survival: Application to proliferation and cytotoxicity assays. Journal of Immunological Methods 65, 55–63.
Nagumo, T., Nishino, T., 1996. Fucan sulfates and their anticoagulant activities. In: Dumitriu, S. (Ed.), Polysaccharides in medicinal applications. Marcel Dekker, New York, pp. 545–574.
Nakajima, A., Matsuda, E., Masuda, Y., Sameshima, H., Ikenoue, T., 2012. Characteristics of the spin-trapping reaction of a free radical derived from AAPH: Further development of the ORAC-ESR assay. Analytical and Bioanalytical Chemistry 403, 1961–1970.
Nguyen, T.L., Wang, D., Hu, Y., Fan, Y., Wang, J., Abula, S., et al., 2012. Immuno-enhancing activity of sulfated Auricularia auricula polysaccharides. Carbohydrate Polymers 89 (4), 1117–1122.
Painter, T.J., 1983. Algal polysaccharides. In: Aspinall, E.O. (Ed.), The polysaccharides, vol. II. Academic Press, Orlando, pp. 157–285.
Panikkar, R., Brasch, D.J., 1996. Composition and block structure of alginates from New Zealand brown seaweeds. Carbohydrate Research 293, 119–132.
Patankar, M.S., Oehninger, S., Barnett, T., Williams, R.L., Clark, G.F., 1993. A revised structure for fucoidan may explain some of its biological activities. Journal of Biological Chemistry 268 (29), 21770–21776.
Percival, E.E., Venegas Jara, M.F., Weigel, H., 1983. Carbohydrates of the brown seaweeds Lessonia nigrescens. Phytochemistry 22 (6), 1429–1432.
Pérez-Cruz, K., Moncada-Basualto, M., Morales-Valenzuela, J., Barriga-González, G., Navarrete-Encina, P., Núñez-Vergara, L., et al., 2017. Synthesis and antioxidant study of new polyphenolic hybrid-coumarins. Arabian Journal of Chemistry https://doi.org/10.1016/j.arabjc.2017.05.007.
Pérez-Molina, J.A., Molina, I., 2018. Chagas disease. The Lancet 391 (10115), 82–94.
Pomin, V.H., Mourão, P.A.S., 2008. Structure, biology, evolution and medical importance of sulfated fucans and galactans. Glycobiology 18, 1016–1027.
Rendleman, J.A., 1978. Metal-polysaccharide complexes—Part I. Food Chemistry 3 (1), 47–79.
Reyes, M.E., 2011. Licentiate in biochemistry thesis, universidad de Santiago de Chile, Chile. Universidad de Santiago de Chile, Santiago, 1–50.
Ringgeler, S., Kappes, B., 2016. Antiparasitics from algae. In: Müller, S., Cerdan, R., Radulescu, O., Selzer, P.M. (Eds.), Comprehensive analysis of parasite biology: From metabolism to drug discovery. Wiley-Blackwell, New Jersey, pp. 41–74.
Robledo-O'Ryan, N., Matos, M.J., Vazquez-Rodriguez, S., Santana, L., Uriarte, E., Moncada-Basualto, M., et al., 2017. Synthesis, antioxidant and antichagasic properties of a selected series of hydroxy-3-arylcoumarins. Bioorganic Medicinal Chemistry 25, 621–632.
Spavieri, J., Kaiser, M., Casey, R., Hingley-Wilson, S., Lalvani, A., Blunden, G., et al., 2010. Antiprotozoal, antimycobacterial and cytotoxic potential of some british green algae. Phytotherapy Research 24 (7), 1095–1098.
Sudharsan, S., Subhapradha, N., Seedevi, P., Shanmugam, V., Madeswaran, P., Shanmugam, A., et al., 2015. Antioxidant and anticoagulant activity of sulfated polysaccharide from Gracilaria debilis (Forsskal). International Journal of Biological Macromolecules 81, 1031–1038.
Torres, F.A.E., Passalacqua, T.G., Velásquez, A.M.A., de Souza, R.A., Colepicolo, P., Graminha, M.A.S., 2014. New drugs with antiprotozoal activity from marine algae: A review. Revista Brasileira de Farmacognosia 24 (3), 265–276.
Venegas, M., Matsuhiro, B., Edding, M.E., 1993. Alginate composition of Lessonia trabeculata (phaeophyta: Laminariales) growing in exposed and sheltered habitats. Botanica Marina 36, 47–59.
Villamena, F.A., 2017. Reactive species detection in biology. From fluorescence to electron paramagnetic resonance spectroscopy, 1st ed. Elsevier, Boston, (Chapter 5).
Wijesinghe, W.A.J.P., Jeon, Y.-J., 2012. Biological activities and potential industrial applications of fucose rich sulfated polysaccharides and fucoidans isolated from brown seaweeds: A review. Carbohydrate Polymers 88, 13–20.
Xu, Y., Gao, Y., Liu, F., Niu, X., Wang, L., Li, X., et al., 2017. Sulfated modification of the polysaccharides from blackcurrant and their antioxidant and α-amylase inhibitory activities. International Journal of Biological Macromolecules https://doi.org/10.1016/j.ijbiomac.2017.11.164.
Yu, Y., Shen, M., Song, Q., Xie, J., 2018. Biological activities and pharmaceutical applications of polysaccharide from natural resources: A review. Carbohydrate Polymers 183, 91–101.
Yu, Y., Shen, M., Wang, Z., Wang, Y., Xie, M., Xie, J., 2017. Sulfated polysaccharide from Cyclocarya paliurus enhances the immunomodulatory activity of macrophages. Carbohydrate Polymers 174, 669–676.